Metal Complexes with Tetrapyrrole Ligands, LXI[1]

Structure and Products of Electrochemical Oxidation of Zirconium(IV) and Hafnium(IV) Bisporphyrinate Double-Deckers

Johann W. Buchler*[a], André De Cian[b], Steffen Elschner[c], Jean Fischer[b], Peter Hammerschmitt[a], and Raymond Weiss*[b]

Institut für Anorganische Chemie, Technische Hochschule Darmstadt[a],
Hochschulstraße 10, W-6100 Darmstadt, F.R.G.

Laboratoire de Cristallochimie et de Chimie Structurale au CNRS (URA 424), Université Louis Pasteur[b],
4, rue Blaise Pascal, F-67070 Strasbourg Cedex, France

Angewandte Physik, Hoechst AG[c],
W-6230 Frankfurt am Main 80, F.R.G.

Received July 19, 1991

Key Words: Zirconium porphyrins / Hafnium porphyrins / Porphyrin double-deckers / Metal bisporphyrinates

The electrochemical oxidation of zirconium and hafnium double-deckers $M(P)_2$ (M = Zr, Hf; P = OEP, TPP) (Scheme 1)[2] leads to mono- and dications which show near infrared absorption bands which are of $\approx 2000\ cm^{-1}$ higher energy than those of the corresponding cerium double-decker cations. $[Zr(OEP)_2]X$, $[Zr(OEP)_2]X_2$, and $[Zr(TPP)_2]X$ (X = ClO_4^- and PF_6^-) are isolated after electrochemical oxidation and are characterized by IR and NMR spectroscopy. Magnetic susceptibility measurements (2 K < T < 300 K) of the solids confirm the strong coupling of the electron spins in the diamagnetic dication salt $[Zr(OEP)_2][ClO_4]_2$. The molecular structure of $Zr(OEP)_2$ is elucidated by an X-ray structural analysis.

Sandwich complexes $M(P)_2$ (Scheme 1) with tetravalent metal ions are known for cerium[3,4] and uranium and thorium[5] since several years, whereas zirconium and hafnium bisporphyrinates have been reported only recently[6,7]. The cathodic shifts of the oxidation potentials and the blue-shift of the near infrared absorption bands of the mono- and diradical cations $[M(P)_2]^{n+}$ (M = Zr, Hf; P = OEP, TPP; n = 1, 2) of these compounds as compared with the analogous cerium complexes are interpreted in terms of an increased interaction of the π-electron systems of the porphyrin ligands due to the smaller ionic radii of zirconium and hafnium. Continuing our work on zirconium and hafnium bisporphyrinates, we report here on the crystal and molecular structure of zirconium bis(octaethylporphyrinate), $Zr(OEP)_2$, one of the starting materials, and especially on the detailed characterization of the mono- and diradical cation salts of zirconium and hafnium bisporphyrinates, $[M(P)_2]^{n+}[X^-]_n$ (M = Zr, Hf; P = TPP, OEP; X = ClO_4, PF_6; n = 1, 2). Despite numerous attempts, crystals suitable for a determination of the crystal and molecular structure of these salts have not been obtained.

Scheme 1. Neutral, mono- and dicationic metal bis(tetrapyrrole) double-deckers (M = Ce, Hf, Zr; X = ClO_4, PF_6)

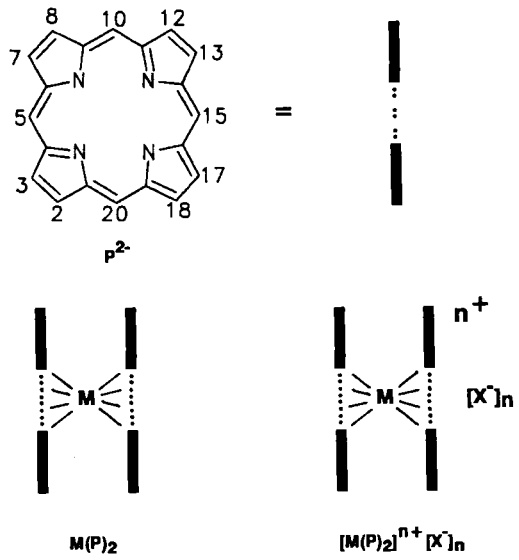

Molecular Structure of $Zr(OEP)_2 \cdot 2\ DMSO$: Single crystals have been grown by slow diffusion of DMSO into a toluene solution of $Zr(OEP)_2$. For details of the structure determination see Table 1 and experimental part[8]. The structure consists of discrete $(Zr(OEP))_2$ double-decker molecules not exhibiting any bonding interactions with one another and the two DMSO solvate molecules. Figure 1 shows the ORTEP plot of one double-decker unit, Figure 2 the perpendicular displacements of the metal and the porphyrin

Specification of the tetrapyrrole systems used

$H_2(P)$	Compound
$H_2(TPP)$	5,10,15,20-Tetraphenylporphyrin
$H_2(TTP)$	5,10,15,20-Tetrakis(4-methylphenyl)porphyrin
$H_2(OEP)$	2,3,7,8,12,13,17,18-Octaethylporphyrin
$H_2(Pc)$	Phthalocyanine

  0009–2940/92/0101–0107 $ 3.50+.25/0

Table 1. Crystallographic data of $Zr(OEP)_2 \cdot 2$ DMSO

$C_{76}H_{100}N_8O_2S_2Zr$, 1313.04 g/mol; color: blue-violet; crystal system: monoclinic, space group $P2_1/c$; a = 1277.7(3), b = 1979.8(5), c = 2835.5(6) pm; β = 97.73(2) °; V = 7107.5·10^6 pm^3; Z = 4; d(calcd) 1.227 g/cm^3; crystal size: 0.20 x 0.20 x 0.26 mm; diffractometer: Philips PW1100/16, θ/2θ-mode; radiation: Cu-K_α, graphite-monochromated; μ: 21.914 cm^{-1}; temperature: 173 K; scan speed (°/s): 0.024; scan width (°): 0.80 + 0.143 tg(θ); θ limits (°): 3/49; octants: ±h+k+l; number of data collected: 7455; number of data with I>3σ(I): 5655; number of variables refined: 792; R(F): 0.046; R_w(F): 0.078; p: 0.08; GOF: 1.781.

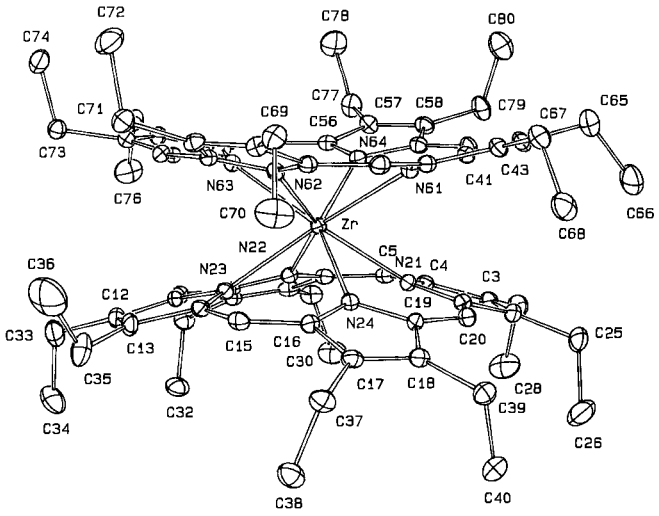

Figure 1. ORTEP plot of one $Zr(OEP)_2$ molecule

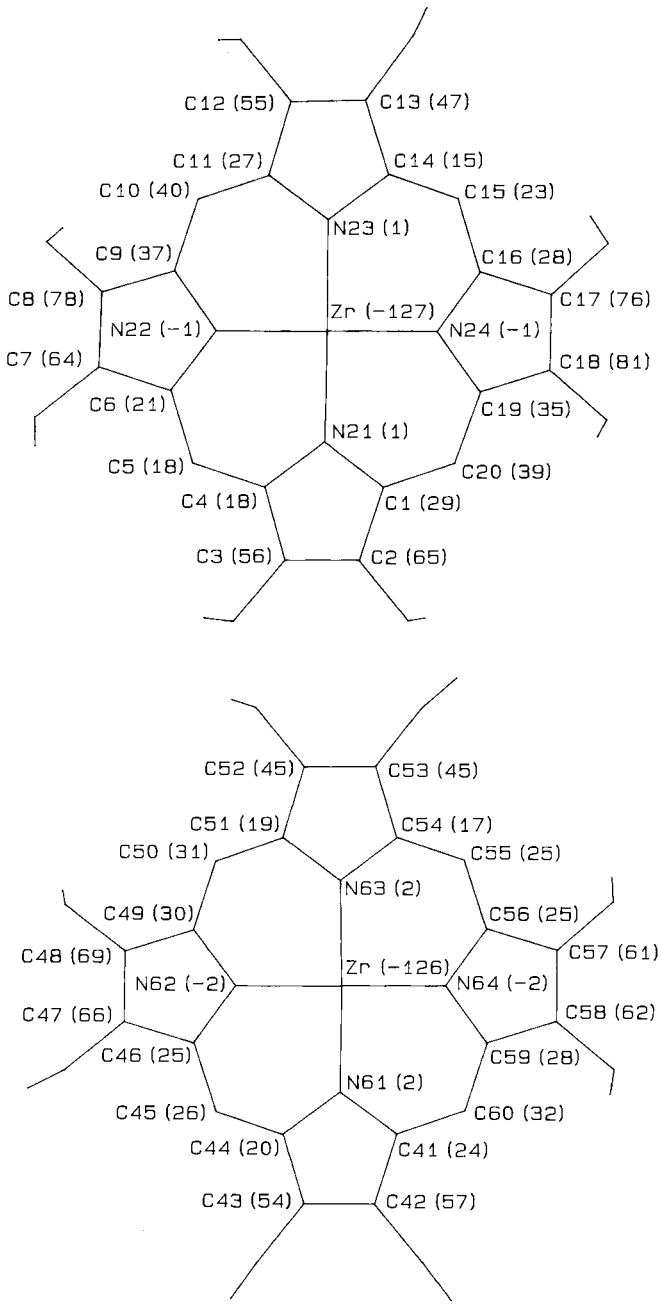

Figure 2. Numbering scheme and perpendicular displacements of the metal and the porphyrin core atoms (in pm) relative to the 24-atom core mean planes of the two porphyrin rings

core atoms (in pm) relative to the 24-atom core mean planes of the two rings with the numbering scheme used for these atoms. Table 2 lists the atomic coordinates for the non-hydrogen atoms. Selected bond lengths and angles are given in Table 3.

The two OEP rings of the double-decker molecule are rotated by an angle of ≈45° with respect to their eclipsed position. The nitrogen atoms set up a slightly distorted square antiprism about the zirconium atom. Since the molecular structure of the analogous compound $Zr(TPP)_2$ has already been determined[6a,7], the data now available for $Zr(OEP)_2$ allow for the first time a comparison of structural features of double-deckers containing OEP and TPP ligands and the same metal ion. We refer to the values of $Zr(TPP)_2 \cdot 4\ H_2O$[6a] since the respective data of $Zr(TPP)_2 \cdot C_5H_{12}$[7] are essentially the same and have been obtained from just isotropically refined carbon positions. Suslick et al.[7] have obtained a solvent-free crystalline modification of $Zr(OEP)_2$ which they report to be isomorphous with $Ce(OEP)_2$[3b] but apparently have not determined the molecular structure.

In $Zr(OEP)_2$, the metal–N_p bond lengths range from 236.8(3) to 239.4(3) pm. The mean value amounts to 238.3(9) pm, which is not significantly different from the corresponding value found in $Zr(TPP)_2$ [239.1(2)[6a], 240(1)[7]]. The zirconium atom is located 127.1 and 126.0 pm above the mean planes of the nitrogen atoms of the two OEP rings, and 162.7 and 157.8 pm above their 24-atom core mean planes, respectively (Table 3 and Figure 2). Being 1.3 to 6.6 pm shorter than the corresponding values found in $Zr(TPP)_2$, these data could indicate a slightly stronger π-π interaction of the porphyrin rings in the OEP double-decker as compared with the TPP derivative. The porphyrin rings in $Zr(OEP)_2$ are severely distorted from planarity, as it is the case with all known structures of sandwich complexes with porphyrin or phthalocyanine ligands. The individual pyrrole rings exhibit dihedral angles with the 24-atom core mean

Table 2. Fractional atomic coordinates[a,b] and equivalent thermal parameters[c] for $Zr(OEP)_2 \cdot 2\ DMSO$[d]

Atom	x	y	z	B(Å²)	Atom	x	y	z	B(Å²)
ZR	0.25087(3)	0.24774(2)	0.35413(1)	2.16(1)	C45	-0.0174(4)	0.1730(2)	0.3480(2)	2.9(1)
C1	0.2928(4)	0.1646(3)	0.4593(2)	2.8(1)	C46	0.0121(4)	0.1912(2)	0.3044(2)	2.6(1)
C2	0.3384(4)	0.1726(3)	0.5084(2)	3.4(1)	C47	-0.0508(4)	0.1754(2)	0.2590(2)	2.9(1)
C3	0.4047(4)	0.2261(3)	0.5098(2)	3.3(1)	C48	-0.0044(4)	0.2088(2)	0.2258(2)	2.8(1)
C4	0.4003(4)	0.2495(2)	0.4615(2)	2.8(1)	C49	0.0851(4)	0.2437(2)	0.2502(2)	2.4(1)
C5	0.4691(4)	0.2979(3)	0.4476(2)	3.0(1)	C50	0.1479(4)	0.2877(2)	0.2282(2)	2.7(1)
C6	0.4902(4)	0.3080(2)	0.4021(2)	2.8(1)	C51	0.2220(4)	0.3315(2)	0.2497(2)	2.3(1)
C7	0.5838(4)	0.3410(2)	0.3904(2)	3.2(1)	C52	0.2709(4)	0.3842(2)	0.2250(2)	2.8(1)
C8	0.5867(4)	0.3298(3)	0.3431(2)	3.0(1)	C53	0.3255(4)	0.4243(2)	0.2589(2)	2.9(1)
C9	0.4927(4)	0.2934(2)	0.3262(2)	2.4(1)	C54	0.3098(4)	0.3950(2)	0.3044(2)	2.7(1)
C10	0.4688(4)	0.2722(3)	0.2797(2)	2.9(1)	C55	0.3422(4)	0.4254(2)	0.3474(2)	2.7(1)
C11	0.3923(4)	0.2268(3)	0.2625(2)	2.6(1)	C56	0.3131(4)	0.4074(2)	0.3908(2)	2.8(1)
C12	0.3852(4)	0.1980(3)	0.2159(2)	3.2(1)	C57	0.3320(4)	0.4493(3)	0.4334(2)	3.2(1)
C13	0.3097(4)	0.1500(3)	0.2129(2)	3.3(1)	C58	0.2829(4)	0.4175(3)	0.4667(2)	3.4(1)
C14	0.2706(4)	0.1490(2)	0.2587(2)	2.7(1)	C59	0.2354(4)	0.3571(2)	0.4450(2)	2.8(1)
C15	0.2077(4)	0.0995(2)	0.2731(2)	2.9(1)	C60	0.1708(4)	0.3156(3)	0.4671(2)	3.0(1)
C16	0.1916(4)	0.0861(2)	0.3195(2)	2.7(1)	N61	0.1070(3)	0.2420(2)	0.3995(1)	2.52(9)
C17	0.1518(4)	0.0227(2)	0.3346(2)	3.0(1)	N62	0.0958(3)	0.2324(2)	0.2982(1)	2.42(8)
C18	0.1580(4)	0.0258(2)	0.3828(2)	2.8(1)	N63	0.2494(3)	0.3373(2)	0.2985(1)	2.45(8)
C19	0.1995(4)	0.0910(2)	0.3964(2)	2.6(1)	N64	0.2562(3)	0.3501(2)	0.3989(1)	2.51(9)
C20	0.2291(4)	0.1113(3)	0.4427(2)	3.3(1)	C65	0.0013(5)	0.2451(3)	0.5171(2)	4.6(2)
N21	0.3302(3)	0.2129(2)	0.4305(1)	2.46(9)	C66	0.0643(6)	0.2042(5)	0.5539(2)	7.4(2)
N22	0.4326(3)	0.2800(2)	0.3620(1)	2.64(9)	C67	-0.1213(4)	0.1473(3)	0.4379(2)	3.9(1)
N23	0.3201(3)	0.1982(2)	0.2880(1)	2.51(9)	C68	-0.0941(5)	0.0741(3)	0.4470(2)	5.0(1)
N24	0.2197(3)	0.1287(2)	0.3575(1)	2.51(9)	C69	-0.1440(4)	0.1293(3)	0.2523(2)	3.6(1)
C25	0.3193(5)	0.1260(3)	0.5481(2)	4.8(1)	C70	-0.1097(5)	0.0564(3)	0.2488(3)	5.7(2)
C26	0.3897(7)	0.0638(4)	0.5524(3)	7.3(2)	C71	-0.0443(4)	0.2114(3)	0.1734(2)	3.5(1)
C27	0.4763(6)	0.2538(3)	0.5516(2)	5.0(2)	C72	-0.1221(6)	0.2668(4)	0.1597(2)	5.7(2)
C28	0.5875(6)	0.2243(4)	0.5562(3)	7.2(2)	C73	0.2599(4)	0.3917(3)	0.1721(2)	3.2(1)
C29	0.6664(4)	0.3756(3)	0.4259(2)	4.1(1)	C74	0.1641(5)	0.4309(3)	0.1515(2)	4.8(1)
C30	0.7482(5)	0.3288(4)	0.4502(3)	6.1(2)	C75	0.3867(4)	0.4867(3)	0.2524(2)	3.9(1)
C31	0.6751(4)	0.3437(3)	0.3151(2)	4.0(1)	C76	0.5024(5)	0.4773(4)	0.2601(3)	6.3(2)
C32	0.7454(5)	0.2815(3)	0.3124(2)	5.3(2)	C77	0.3879(5)	0.5153(3)	0.4362(2)	4.5(1)
C33	0.4559(5)	0.2155(3)	0.1791(2)	4.8(1)	C78	0.3197(6)	0.5747(3)	0.4183(3)	6.5(2)
C34	0.5618(5)	0.1800(4)	0.1865(2)	7.1(2)	C79	0.2749(5)	0.4409(3)	0.5164(2)	4.5(1)
C35	0.2777(5)	0.1033(4)	0.1721(2)	5.5(2)	C80	0.1739(6)	0.4764(4)	0.5211(2)	6.7(2)
C36	0.1945(9)	0.1263(5)	0.1427(3)	10.7(3)	S1	0.4128(2)	0.6187(1)	0.13854(7)	7.48(5)
C37	0.1268(4)	-0.0373(3)	0.3027(2)	3.6(1)	O1	0.3238(4)	0.5729(3)	0.1413(2)	8.8(1)
C38	0.2256(5)	-0.0748(3)	0.2921(2)	4.7(1)	C81	0.4165(6)	0.6347(4)	0.0782(3)	8.6(2)
C39	0.1358(4)	-0.0288(3)	0.4159(2)	3.8(1)	C82	0.5281(6)	0.5708(5)	0.1479(3)	9.0(2)
C40	0.2323(5)	-0.0724(3)	0.4332(2)	5.5(2)	S2	0.0551(2)	0.5482(2)	0.6506(1)	11.53(8)
C41	0.1073(4)	0.2642(3)	0.4457(2)	3.0(1)	O2'	0.1492(6)	0.5451(5)	0.6353(4)	9.1(3)
C42	0.0241(4)	0.2318(3)	0.4674(2)	3.3(1)	O2"	0.112(1)	0.5055(8)	0.6790(5)	12.6(4)*
C43	-0.0281(4)	0.1911(3)	0.4335(2)	3.0(1)	C83	-0.0037(6)	0.6134(4)	0.6754(4)	9.0(2)
C44	0.0223(4)	0.1988(2)	0.3915(2)	2.6(1)	C84	-0.0451(7)	0.5195(6)	0.6142(4)	12.2(3)

[a] Figure 2 displays the numbering scheme of all non-hydrogen atoms other than C81–84; O1, O2, S1, and S2 refer to the DMSO molecules. – [b] The estimated standard deviations of the last significant digits are given in parentheses. – [c] Anisotropically refined atoms are given as isotropic equivalent displacement parameters defined as $(4/3) \cdot [a^2 \cdot \beta(1,1) + b^2 \cdot \beta(2,2) + c^2 \cdot \beta(3,3) + ab(\cos\gamma) \cdot \beta(1,2) + ac(\cos\beta) \cdot \beta(1,3) + bc(\cos\alpha) \cdot \beta(2,3)]$. – [d] The positions of the O atom of the disordered DMSO molecule are denoted by O2′ and O2″, respectively (see *)

planes between 12.3 and 19.9°, the mean value amounts to 16°. A comparison with the corresponding data found in $Zr(TPP)_2$ (10.0, 23.6, and 17.0°) shows that the TPP rings are domed and ruffled to a slightly larger extent than the OEP rings. This might be due to sterical interactions between the bulky phenyl groups of the TPP ligand. It should be taken into account, however, that *meso*-tetraarylporphyrins generally tend to deviate more from planarity than the octaethyl-substituted ligand does[9]. The smaller extent of doming and ruffling of the porphyrin in $Zr(OEP)_2$ as

Table 3. Selected bond lengths [pm] and bond angles [°] of Zr(OEP)$_2$. [C_α, C_β, C_m, C_α(Et), and C_β(Et) denote the α and β carbon atoms of the pyrrole ring, the methine carbon, and the two carbon atoms of the ethyl group, respectively]

Bonds		Core bond lengths	
Zr-N	236.8(3) 238.3(3)	NC_α	137.8(5)
	239.0(3) 238.4(3)	$C_\alpha C_\beta$	144.2(9)
	238.8(3) 237.2(3)	$C_\beta C_\beta$	135.7(6)
	239.4(3) 238.6(3)	$C_\alpha C_m$	137.7(9)
		$C_\beta C_\alpha$(Et)	149.7(8)
mean value: 238.3(9)		C_α(Et)C_β(Et)	150(4)

Core bond angles			
$C_\alpha NC_\alpha$	104.3(5)	$C_\alpha C_m C_\alpha$	126.6(9)
$NC_\alpha C_\beta$	111.3(5)	$NC_\alpha C_m$	124.6(5)
$C_\alpha C_\beta C_\beta$	106.4(4)	$C_\beta C_\alpha C_m$	123.6(5)

Least squares planes distances	$Zr(OEP)_2$	$Zr(TPP)_2$	$Ce(OEP)_2$
$d(N_4N_4)$	253.1	256.8	275.2
$d(C_{20}N_4\text{-}C_{20}N_4)$	320.5	328.4	340.6
$d(C_{20}N_4\text{-}N_4)$	35.6/31.7	35.8	31.5/33.9

compared with $Zr(TPP)_2$ therefore should not be regarded as being specific to the double-decker.

In conclusion, the rather small differences between the molecular structures of $Zr(OEP)_2$ and $Zr(TPP)_2$ demonstrate that the bulky phenyl groups of the TPP ligand do not account for a significantly increased repulsion of the two porphyrin rings in the double-decker molecule as compared with the smaller ethyl groups of the OEP ligand.

Electrochemical Oxidations and UV/Vis/NIR Spectra: Solutions of the sandwich compounds $M(P)_2$ (M = Zr, Hf; P = OEP, TPP) in CH_2Cl_2 have been electrolyzed under coulometric control to give the mono- and dications, respectively, at the voltages indicated (eq. 1), for details see experimental part. Figures 3 and 4 show the UV/Vis/NIR spectra for $Zr(OEP)_2$ or $Zr(TPP)_2$ and the respective mono- and dications.

$$\underset{\text{P=OEP: } +0.40\,\text{V}}{M(P)_2} \xrightarrow{-e^-} \underset{\text{P=TPP: } +0.75\,\text{V}}{[M(P)_2]^+} \xrightarrow[+0.80\,\text{V}\ (+1.25\,\text{V})]{-e^-} [M(P)_2]^{2+} \quad (1)$$

(versus SCE; $LiClO_4$ or KPF_6).

The formation of the cations according to eq. (1) is a reversible process. This has been shown before by cyclic voltammetry[6,7]. As compared with the spectra of the neutral complexes, the monocations $[M(P)_2]^+$ show blue-shifted Soret bands and only weak absorptions between 400 and 800 nm. In the near infrared (NIR) region the cations exhibit new broad and intense absorptions being characteristic of metal(IV) bisporphyrinates with oxidized ligands[3c,6a,10]. The dications exhibit Soret and NIR bands that are blue-shifted with respect to the monocations. The UV/Vis/NIR absorption maxima are compiled in Table 4.

NIR bands likewise appear in lanthanoid(III) bisporphyrinate double-deckers having oxidized porphyrin ligands[11]. The energies of the NIR bands of the lanthanoid bisporphyrinate monoradicals $Ln(OEP)_2$[11a,b], $Ln(TPP)_2$[12] and the diradical cations $[Ln(TPP)_2]^+$[12] have been shown to be dependent on the ionic radii of the lanthanoid ions and the "oxidation state" of the double-decker molecule. A linear correlation between the ionic radii and the energies of the NIR bands has been observed in the OEP[11a] and the TPP[12] series, and the cations $[Ln(P)_2]^+$ show always NIR bands blue-shifted to those of the neutral species $Ln(P)_2$. As examples for this observation, the values of the oxidation products of $[Y(OEP)_2]^-$[13], $[Pr(OEP)_2]^-$[11e] and $[Pr(TPP)_2]^-$[12] are given in Table 5.

As a whole, in Table 5 the spectral properties of a series of OEP and TPP double-deckers are compared in which the coupled π-electron systems of two cofacially oriented porphyrin rings are lacking one or two electrons, and which are each ordered according to an increasing ionic radius r_i of the octacoordinated metal ions, respectively. The distances of the 24-atom core mean planes are also given in those cases where crystal structures have been determined.

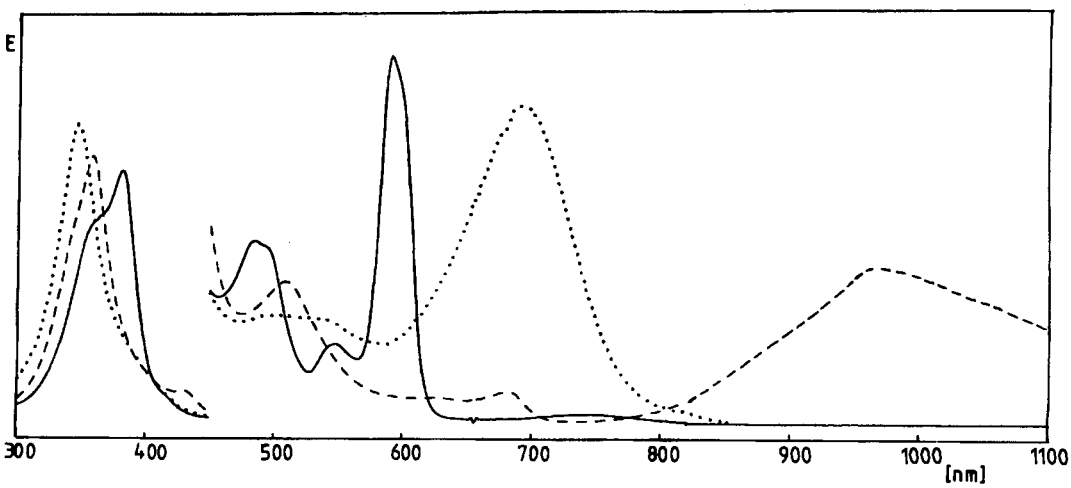

Figure 3. Electrochemical oxidation of $Zr(OEP)_2$ followed by UV/Vis/NIR spectra. —— $Zr(OEP)_2$; – – – $[Zr(OEP)_2]PF_6$; ··· $[Zr(OEP)_2][PF_6]_2$

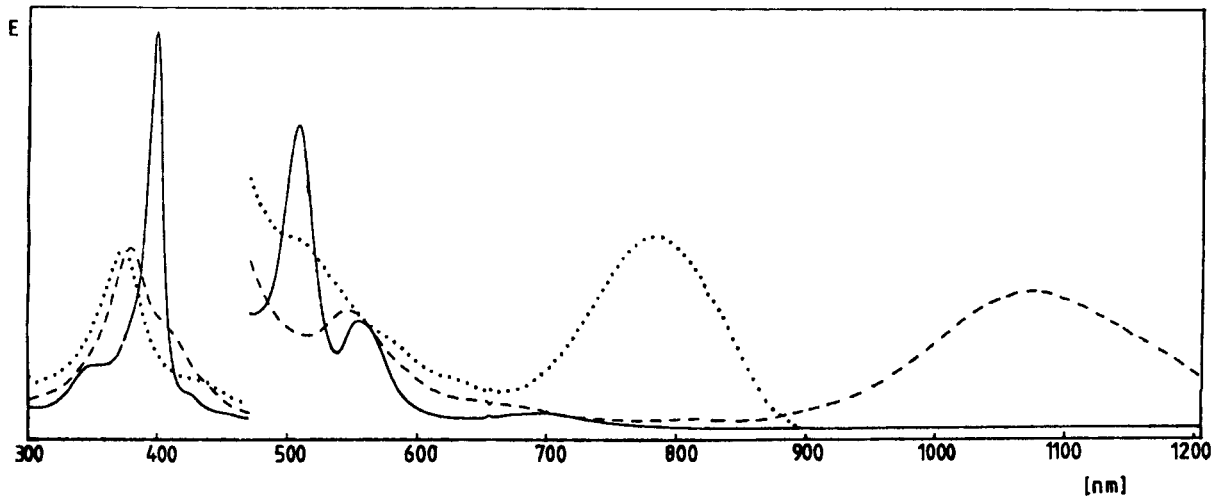

Figure 4. Electrochemical oxidation of $Zr(TPP)_2$ followed by UV/Vis/NIR spectra. —— $Zr(TPP)_2$; – – – $[Zr(TPP)_2]PF_6$; ··· $[Zr(TPP)_2][PF_6]_2$

Table 4. Comparison of the UV/Vis/NIR spectra of the neutral and oxidized metal(IV) bisporphyrinates $M(P)_2$, $[M(P)_2]^+$, and $[M(P)_2]^{2+}$; (λ_{max} [nm], lgε in parentheses)

Complex	Soret	IV	III	II	I	NIR
$Zr(OEP)_2$	382	490	550	592	750	
	(5.22)	(4.10)	(3.78)	(4.39)	(2.72)	
$[Zr(OEP)_2]^+$	358	430	508	684		966
	(5.20)	(4.36)	(3.93)	(3.35)		(3.93)
$[Zr(OEP)_2]^{2+}$	346					692
	(5.25)					(4.27)
$Hf(OEP)_2$	380	486	548	592	750	
	(5.18)	(4.04)	(3.67)	(4.31)	2.69)	
$[Hf(OEP)_2]^+$	356	428	508	684		958
	(5.21)	(4.43)	(3.94)	(3.37)		(3.91)
$[Hf(OEP)_2]^{2+}$	344					684
	(5.28)					(4.24)
$Zr(TPP)_2$	396		506	554	696	
	(5.54)		(4.42)	(3.97)	(3.15)	
$[Zr(TPP)_2]^+$	378			546		1074
	(5.19)			(4.01)		(4.00)
$[Zr(TPP)_2]^{2+}$	372					784
	(5.19)					(4.22)
$Hf(TPP)_2$	394		506	554	700	
	(5.57)		(4.45)	(4.00)	(3.19)	
$[Hf(TPP)_2]^+$	376			546		1054
	(5.23)			(4.04)		(4.05)
$[Hf(TPP)_2]^{2+}$	370					768
	(5.21)					(4.25)

Table 5. Comparison of the maxima of the Vis/NIR bands (CH_2Cl_2, λ_{max} [nm]) of the oxidation products of the double-decker species $M^{IV}(P)_2$ and $[M^{III}(P)_2]^-$. Column **A**: maxima of the products of one-electron oxidation, $[M^{IV}(P)_2]^+$ or $M^{III}(P)_2$; column **B**: maxima of the products of two-electron oxidation, $[M^{IV}(P)_2]^{2+}$ and $[M^{III}(P)_2]^+$. The ionic radii r_i of the central metals[18] in the double-deckers and the ring-ring distances d_{r-r} are also given (in pm)

	A	B	r_i	d_{r-r}	Ref.
$Hf(OEP)_2$	958	684	83		6
$Zr(OEP)_2$	966	692	84	320	6
$Ce(OEP)_2$	1280	808	97	340	3c,6b,8a
$[Y(OEP)_2]^-$	1175	816	102		11c,13
$[Eu(OEP)_2]^-$	1280		107	342	11d
$[Pr(OEP)_2]^-$	1400	920	114		11e
2 Zn(OEP) [a]	---	930 [a]	--	331	14
$Hf(TPP)_2$	1054	768	83		6
$Zr(TPP)_2$	1074	784	84	328	6
$Ce(TPP)_2$	1350	1017	97		6b
$U(TPP)_2$	1270	990	100		5b
$Th(TPP)_2$	1480	1080	106	347	5b
$[Pr(TPP)_2]^-$	1500	1140	114		12

[a] Data of $[Zn(OEP)]_2^{2+}$ prepared by two-electron oxidation of two Zn(OEP) molecules.

Also enclosed in Table 5 is the NIR maximum of the diamagnetic dication $[Zn(OEP)]_2^{2+}$ [14] which is formed on cooling of solutions of the paramagnetic zinc(II) porphyrin π-radical monocation $Zn(OEP)^+$ [14a,b]. The crystal structure of the diaqua bisperchlorate salt of this cation, $[(H_2O)Zn(OEP)]_2[ClO_4]_2$, has been determined[14c]. The two porphyrin rings are planar and held together coaxially at a distance of 331 pm by strong π-π interactions. The cation $[Zn(OEP)]_2^{2+}$ fully corresponds to the series of doubly oxidized double-deckers mentioned in Table 5. [The π-radical cation $Zn(OEP)^+$ does not have a NIR band because it is just a monoporphyrin.] The analogy of the ^{1}H-NMR and NIR spectra of $[Zn(OEP)]_2^{2+}$ and $[Ln(OEP)_2]^+$ (Ln = Pr, Y) has been noted earlier[11e,13].

Since Zr^{IV} and Hf^{IV} have the smallest ionic radii of the compounds compared in Table 5, the ring-ring distances in the corresponding double-deckers are the smallest, and the NIR bands of the oxidation products have the smallest values. As already observed in the Ln^{III} series, the NIR bands

are blue-shifted on abstraction of the second electron from the coupled π-electron system.

The NIR bands of the TPP series are red-shifted with respect to those of the OEP system. Furthermore, the ring-ring distance of $Zr(OEP)_2$ is smaller than that of $Zr(TPP)_2$. These observations indicate a stronger π-π interaction in the OEP double-deckers. – The NIR bands generally are hypsochromically shifted when Zr is replaced by Hf. This reflects the minimally smaller ionic radius of the Hf^{IV} ion. – The series of the M^{IV} ions (Hf, Zr, Ce, Th) and of the M^{III} ions (Y, Eu, Pr) *in Table 5* cannot be strictly compared because the starting molecules of the former or latter series are neutral or negatively charged, respectively. This may alter the energy of the NIR transitions although the ionic radii are equal.

Since the properties of the series $M(P)_2/M(P)_2^+/M(P)_2^{2+}$ with M = Zr, Hf fit well into the other well-established species having comparable electronic configurations of the porphyrin rings, the identification of these cations seems clearly established. Further evidence for their existence is presented in the following section.

Some exceptions may be noted for the actinoid double-deckers. Contrary to the cation salts of zirconium and hafnium bisporphyrinates reported here, the mono- and dications of $Th(TPP)_2$ and $U(TPP)_2$[5b] show two surprising features: first, the Soret bands of the dications are red-shifted to those of the monocations and not blue-shifted as it is the case with all other bisporphyrinates. In addition, the NIR bands of the cations of $U(TPP)_2$ are blue-shifted to those of the corresponding cerium compounds whereas a red shift is expected due to the larger ionic radius of the uranium ion. The authors give no explanation for this unusual behavior. Possibly $U(TPP)_2$ suffers a metal-centered oxidation, as has been observed in the case of the phthalocyanine compound $U(Pc)(acac)_2$[15]. This might explain at least the blue-shift of the NIR bands.

Isolation and Further Characterization of Salts of the Double-Decker Cations $[M(P)_2]^{n+}$ (M = Zr, Hf; n = 1, 2)

The salts $[Zr(OEP)_2]X$, $[Zr(OEP)_2]X_2$, and $[Zr(TPP)_2]X$ ($X = PF_6^-$ and ClO_4^-) were prepared by electrochemical oxidation of the neutral species in $CH_3CN/LiClO_4$ or CH_3CN/KPF_6 and isolated as solids in amounts of about 30 mg. On redissolution, these salts gave the same UV/Vis/NIR spectra that were given in Table 4.

As it has been observed for the redox potentials[6a], the energies of the NIR absorptions of the Zr and Hf bisporphyrinate double-deckers clearly show the effect of the stronger coupling of the π-electron systems due to the smaller ionic radii of Zr^{IV} and Hf^{IV} as compared with the analogous Ce^{IV} or Th^{IV} complexes[6c].

Infrared Spectra: The infrared spectra of the compounds $[Zr(P)_2]X$ and $[Zr(P)_2]X_2$ were run in nujol mulls to avoid the reduction of the cationic species occurring in KBr pellets. Besides the absorptions of the ClO_4^- or PF_6^- anions the spectra show the characteristic "oxidation state marker bands" (OM) of porphyrin π-radicals[16]. $[Zr(OEP)_2]X$ shows three absorptions at 1630, 1610, and 1555 cm^{-1} which are absent in $Zr(OEP)_2$, whereas $[Zr(OEP)_2]X_2$ exhibits one broad absorption at 1575 cm^{-1}. $[Zr(TPP)_2]X$ shows new bands at 1680, 1565, 1510, and 1325 cm^{-1}. Similar effects have been observed in the IR spectra of cerium bisporphyrinate double-decker cation salts[3c,10a].

^{1}H-NMR-Spectra: The ^{1}H-NMR spectrum of $[Zr(OEP)_2]ClO_4$ shows only one broad signal at δ = 3.3 which can be assigned to the methyl protons whereas the signals of the methylene and methine protons are too broad to be observed. This indicates the delocalization of the unpaired electron over the two porphyrin systems as found for other bisporphyrinate radicals[11c–f,17]. In the presence of the spin-relaxer tBu_2NO[18] the signals of the methylene protons can be observed whereas the signal of the methine protons remains undetectable. $[Zr(OEP)_2]^+$, therefore, behaves just as the isoelectronic species $Y(OEP)_2$ and $Lu(OEP)_2$[11c] (Table 6).

Table 6. ^{1}H-NMR signals of $[Zr(OEP)_2]ClO_4$, $Lu(OEP)_2$, and $Y(OEP)_2$ in the presence of tBu_2NO; δ values (half width in Hz)

Complex	CH_3	CH_2	CH_2	CH	Ref.
$[Zr(OEP)_2]ClO_4$	4.40(68)	16.5(525)	27.0(2000)	/	a)
$Y(OEP)_2$	3.16(68)	14.5(110)	22.3(150)	26.8(125)	13a
$Lu(OEP)_2$	3.06(68)	15.0(243)	23.0(414)	30.1(701)	13a

a) This work.

The ^{1}H-NMR spectrum of $[Zr(TPP)_2]ClO_4$ exhibits only one very broad signal between δ = 7 and 11, indicating again a complete delocalization of the unpaired electron including the phenyl rings. $[Th(TPP)_2]SbCl_6$ behaves similarly[5b], whereas in the case of cerium bis(tetraarylporphyrinate) cation salts signals of the phenyl protons have been reported[10a]. The spin relaxer tBu_2NO cannot be used with $[Zr(TPP)_2]ClO_4$ because it quantitatively reduces the latter to neutral $Zr(TPP)_2$.

The dication derived from $Zr(OEP)_2$ may be regarded as a diradical as indicated by the formula $[Zr^{4+}(OEP^{-\bullet})_2]^{2+}$. However, in several other sandwich complexes with two oxidized tetrapyrrole ligands the electron spins seem to be strongly coupled as shown by NMR evidence in the salts $[Y(OEP)_2]SbCl_6$[13] and $[Pr(OEP)_2][AuI_2]$[11e] and by means of EPR and magnetic susceptibility measurements in $[Lu(Pc)_2]SbCl_6$[19].

The ^{1}H-NMR spectrum of $[Zr(OEP)_2][ClO_4]_2$, however, does not corroborate the expected spin coupling. Only one broad signal is observed indicating the presence of a paramagnetic species. Magnetic susceptibility measurements have been performed to find out whether this is due to a rather weak coupling of the unpaired spins in the dication or to some paramagnetic impurity or to some decomposition in the solvent CD_2Cl_2.

Magnetic Susceptibility: Measurements have been carried out between 2 and 300 K using powdered samples of Zr(OEP)$_2$, [Zr(OEP)$_2$]ClO$_4$, and [Zr(OEP)$_2$][ClO$_4$]$_2$. Figure 5 shows the temperature dependence of the molar susceptibilities of these three compounds (plotted versus $1/T$).

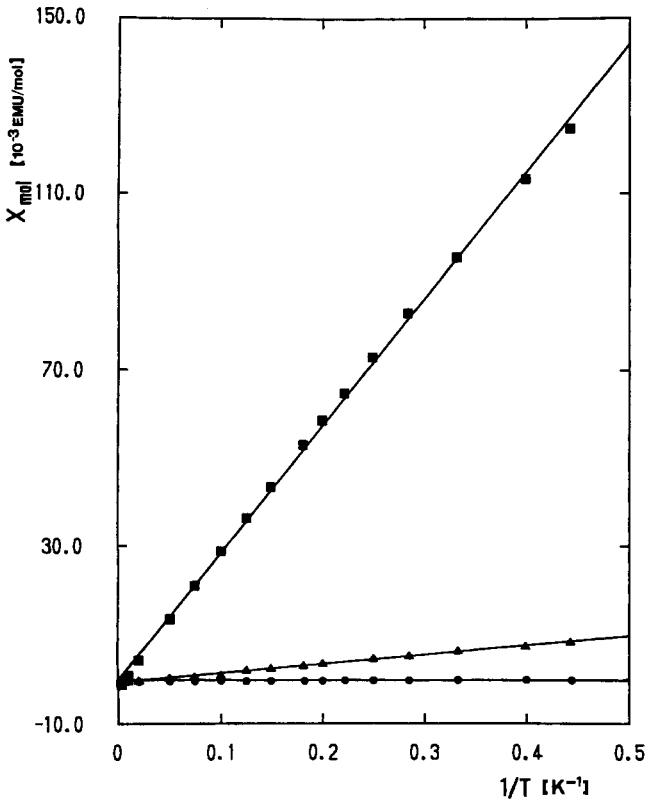

Figure 5. Magnetic susceptibility data:
● Zr(OEP)$_2$; ■ [Zr(OEP)$_2$]ClO$_4$; ▲ [Zr(OEP)$_2$][ClO$_4$]$_2$

As expected, Zr(OEP)$_2$ is diamagnetic with a molar susceptibility of $-499 \cdot 10^{-6}$ emu/mol, being comparable to the value of [Sc(OEP)]$_2$O[20]. This compound is suitable for comparison because the number of electrons of the Sc–O–Sc unit nearly equals that of the zirconium ion.

[Zr(OEP)$_2$]ClO$_4$ is paramagnetic showing Curie behavior in the observed temperature range. The magnetic moment amounts to 1.51 BM and is nearly independent of temperature.

The magnetic properties of [Zr(OEP)$_2$][ClO$_4$] clearly contradict the formulation of this compound as a diradical. There is only a weak paramagnetism which is probably due to a contamination of the sample with a small percentage of a paramagnetic impurity identified as the monocation [Zr(OEP)$_2$]ClO$_4$ by UV/Vis/NIR spectroscopy. This result demonstrates the strong coupling of the unpaired electrons in the [Zr(OEP)$_2$]$^{2+}$ dication. This coupling can be described in terms of qualitative molecular orbital models which have been suggested for porphyrin sandwich complexes[4,6c,12,17]. According to these models the double-decker molecules M^{IV}(P)$_2$ have one HOMO occupied by two electrons. Successive electron abstractions produce an odd-electron species [M^{IV}(P)$_2$]$^+$ and a diamagnetic even-electron species [M^{IV}(P)$_2$]$^{2+}$ with paired spins.

This work was supported by the *Deutsche Forschungsgemeinschaft*. We thank for additional financial contributions from the *Centre National de la Recherche Scientifique* (Paris), the *Fonds der Chemischen Industrie* (Frankfurt), the *Vereinigung von Freunden der Technischen Hochschule Darmstadt*, and the *Otto Röhm Gedächtnisstiftung* (Darmstadt). We thank Professor *J. J. Veith* and Mr. *M. Fischer* for recording the mass spectra, Dr. *S. Braun* for advice on the ^{1}H-NMR spectra, Mr. *U. Mayer* for recording the NMR spectra, and *Bayer AG* for a gift of trichlorobenzene. R. W. thanks the *Alexander-von-Humboldt-Stiftung* for financial support.

Experimental

X-ray Crystallography: Suitable single crystals of Zr(OEP)$_2 \cdot 2$ DMSO were obtained by slow diffusion of DMSO into a toluene solution of Zr(OEP)$_2$ at room temperature. One single crystal was cut from a cluster of crystals. A systematic search in the reciprocal space using a Philips PW 1100/16 automated diffractometer showed that Zr(OEP)$_2 \cdot 2$ DMSO crystallizes in the monoclinic system. Data collection was performed at 173 K. For all calculations the Enraf-Nonius package[21] was used with the exception of a local data reduction program. Three standard reflections measured every hour during data collection showed no significant trend. The raw step-scan data were converted to intensities by using the Lehmann-Larsen method[22] and then corrected for Lorentz and polarization factors. The structure was solved by using the heavy-atom method. After refinement of the heavy atoms, a difference Fourier map revealed maxima of residual electronic density close to the positions expected for hydrogen atoms. They were introduced in structure factor calculations by their computed coordinates (C–H = 0.95 Å) and isotropic temperature factors such as B(H) = 1.3 B_{eqv}(C) Å^2 but not refined. At this stage, empirical absorption corrections were applied using the method of Walker and Stuart[23] since face indexation was not possible under the cold gas stream. The oxygen atom O2 of one of the two DMSO molecules is disordered over two positions in the ratio 1:1 as seen from the difference Fourier synthesis. Full least-squares refinements were done with $\sigma^2(F^2) = \sigma^2_{counts} + (pI)^2$. A final difference map revealed no significant maxima (scattering factor coefficients[24a]; anomalous dispersion coefficients[24b]).

Magnetic Susceptibility Measurements were carried out with a Quantum Design SQUID magnetometer between 2 and 300 K. The accuracy of the experiment was about $50 \cdot 10^{-6}$ emu. The external magnetic field was set to H = 0.5 T. This value was sufficient to obtain large signals and small enough to avoid saturation effects at low temperatures. Powdered samples of Zr(OEP)$_2$, [Zr(OEP)$_2$]ClO$_4$, and [Zr(OEP)$_2$][ClO$_4$]$_2$ with typical masses m = 0.1 g were used. Results are shown in Figure 5.

Methods: MS: Varian MAT 311 A with data system SS 100 MS (direct insertion, ion source at 150°C, field-ion desorption). – IR: Perkin-Elmer 397 (KBr pellets or nujol mulls). – UV/Vis: Spectrophotometer Bruins Instruments Omega 10. – ^{1}H NMR: Spectrometer Bruker WM 300 (300 MHz). – Elemental analyses: Mr. F. Roth, microanalytical laboratory of the Institut für Organische Chemie der TH Darmstadt or Analytische Laboratorien Malissa & Reuter, D-5250 Engelskirchen. The electrochemical equipment and techniques are described elsewhere[11a,15c].

Materials: The following chemicals were purchased from the companies indicated in brackets: [D]chloroform, [D$_2$]dichloromethane, [D$_8$]toluene, lithium perchlorate, potassium hexafluorophosphate (Merck), alumina type W 200 basic super I

(Woelm-ICN-Biomedicals). Acetonitrile (Merck) and dichloromethane (distilled) were passed through an alumina column (super I, basic) prior to use. – The synthesis of the zirconium and hafnium bisporphyrinates is described elsewhere[6].

Electrochemical Oxidation of Zirconium and Hafnium Bisporphyrinates: A solution of about 1 μmol of $M(P)_2$ in 50 ml of CH_2Cl_2/NBu_4PF_6 was electrolyzed first at a potential *a* to give the monocation. A sample for UV/Vis/NIR spectroscopy was taken, and the potential *b* was applied for further oxidation to the dication. The values of the potentials *a* and *b* and the transferred charges for each electrolysis step are compiled in Table 7. For spectroscopic data see Table 4.

Table 7. Applied electrode potentials U_a and U_b and transferred charges Q_a and Q_b for the electrochemical oxidation of $Zr(OEP)_2$, $Zr(TPP)_2$, $Hf(OEP)_2$, and $Hf(TPP)_2$. Potentials in V vs. SCE (Q_a and Q_b in italics; Coulombs and, in parentheses, Faraday per mol)

Complex	[mg(μmol)]	U_a	Q_a	U_b	Q_b
$Zr(OEP)_2$	[1.44 (1.24)]	0.350	*0.102 (0.85)*	0.800	*0.123 (1.03)*
$Hf(OEP)_2$	[1.39 (1.12)]	0.400	*0.078 (0.72)*	0.800	*0.118 (1.09)*
$Zr(TPP)_2$	[1.77 (1.34)]	0.750	*0.112 (0.87)*	1.250	*0.128 (0.99)*
$Hf(TPP)_2$	[1.85 (1.32)]	0.750	*0.116 (0.91)*	1.250	*0.144 (1.13)*

Bis(2,3,7,8,12,13,17,18-octaethylporphyrinato)zirconium(IV) Perchlorate, $[Zr(OEP)_2]ClO_4$: A solution of 30 mg (26 μmol) of $Zr(OEP)_2$ in 50 ml of $CH_3CN/LiClO_4$ was electrolyzed at +0.35 V with simultaneous sonification of the electrolysis cell. Within 2 h, the current dropped from 1.2 to 0.004 mA and 2.46 C (0.98 F/mol) had been transported. After removal of the solvent in vacuo the brown residue was extracted with 50 ml of CH_2Cl_2 and filtered. The filtrate was freed from CH_2Cl_2, the residue was dissolved in 2 ml of CH_2Cl_2, filtered, and 5 ml of toluene was added. Slow evaporation of the solution yielded 30 mg (92%) of dark brown cubes of $[Zr(OEP)_2]ClO_4$. – IR (Nujol), 10 most intense bands + OM bands (OM bands in italics): *1630, 1610, 1555,* 1330, 1090 (ClO_4), 1055, 1015, 980, 955, 840, 720, 690, 620 (ClO_4) cm^{-1}.

$C_{72}H_{88}ClN_8O_4Zr$ (1256.2)
Calcd. C 68.84 H 7.06 Cl 2.82 N 8.92
Found C 66.56 H 7.01 Cl 3.63 N 8.14

The excess of Cl suggested a contamination of the product with $LiClO_4$. Assumption of 1/4 $LiClO_4$ per $[Zr(OEP)_2]ClO_4$ improved the analytical figures:

$C_{72}H_{88}ClN_8O_4Zr \cdot 1/4\,LiClO_4$
Calcd. C 67.41 H 6.91 Cl 3.45 N 8.74
Found C 66.56 H 7.01 Cl 3.63 N 8.14

Bis(2,3,7,8,12,13,17,18-octaethylporphyrinato)zirconium(IV) Hexafluorophosphate, $[Zr(OEP)_2]PF_6$: The synthesis was carried out as described for the perchlorate salt except that KPF_6 was used instead of $LiClO_4$ as supporting electrolyte. – IR (Nujol): same bands as $[Zr(OEP)_2]ClO_4$, bands of PF_6^- at 840 and 560 cm^{-1}.

$C_{72}H_{88}F_6N_8PZr$ (1301.7)
Calcd. C 66.43 H 6.81 F 8.76 N 8.61
Found C 66.63 H 6.55 F 8.27 N 8.23

Bis(2,3,7,8,12,13,17,18-octaethylporphyrinato)zirconium(IV) Diperchlorate, $[Zr(OEP)_2][ClO_4]_2$: A solution of 25 mg (22 μmol) of $Zr(OEP)_2$ in 50 ml of $CH_3CN/LiClO_4$ was electrolyzed at +0.8 V with simultaneous sonification of the electrolysis cell. After the transfer of 3.95 C (1.86 F/mol) the current had dropped from 3 to 0.05 mA, and the electrolysis was stopped. The solvent was removed in vacuo, the green residue extracted with 50 ml of CH_2Cl_2 and filtered.

The filtrate was freed from its solvent. The residue was dissolved in 2 ml of CH_2Cl_2 and filtered. Evaporation of the solvent in vacuo yielded 21 mg (70%) of a dark green powder of $[Zr(OEP)_2][ClO_4]_2$. – IR (Nujol): 10 most intense bands, OM bands in italics: *1575, 1260, 1240,* 1090 (ClO_4), 1055, 1020, 980, 960, 860, 625 (ClO_4) cm^{-1}.

$C_{72}H_{88}Cl_2N_8O_8Zr$ (1355.7) Calcd. C 63.79 H 6.54 N 8.27
Found C 62.18 H 6.35 N 8.31

(Acetonitrile)bis(5,10,15,20-tetraphenylporphyrinato)zirconium(IV) Perchlorate, $[Zr(TPP)_2][ClO_4] \cdot CH_3CN$: A solution of 26 mg (19.4 μmol) of $Zr(TPP)_2$ in 50 ml of $CH_3CN/LiClO_4$ was electrolyzed at +0.750 V with simultaneous sonification of the electrolysis cell. After the transfer of 1.965 C (1.02 F/mol) the current had dropped from 3 to 0.8 mA, and the electrolysis was stopped. The solvent was removed in vacuo. The brown residue was extracted with 30 ml of CH_2Cl_2 and filtered. After removal of the solvent the residue was dissolved in 5 ml of CH_2Cl_2 and filtered. Evaporation of the solvent in vacuo yielded 23 mg (81%) of a black-violet powder of $[Zr(TPP)_2]ClO_4$. – IR (Nujol), 10 most intense bands + OM bands (OM bands in italics): *1680, 1565, 1510,* 1490, 1440, *1325,* 1180, 1090 (ClO_4), 975, 965, 810, 755, 700, 620 (ClO_4) cm^{-1}.

$C_{90}H_{59}ClN_9O_4Zr$ (1457.2) Calcd. C 74.18 H 4.08 N 8.65
Found C 71.78 H 4.10 N 8.66

CAS Registry Numbers

$Zr(OEP)_2$ · 2 DMSO: 137365-84-5 / $[Zr(OEP)_2]ClO_4$: 137365-79-8 / $Zr(OEP)_2$: 132017-20-0 / $[Zr(OEP)_2]PF_6$: 137365-80-1 / $[Zr(OEP)_2][ClO_4]_2$: 137365-81-2 / $[Zr(TPP)_2][ClO_4]$ · CH_3CN: 137365-83-4 / $Zr(TPP)_2$: 133985-31-6 / $[Zr(TPP)_2]^{2+}$: 131618-83-2 / $Hf(OEP)_2$: 132017-18-6 / $[Hf(OEP)_2]^+$: 132017-19-7 / $[Hf(OEP)_2]^{2+}$: 131618-85-4 / $Hf(TPP)_2$: 131618-88-7 / $[Hf(TPP)_2]^+$: 131635-39-7 / $[Hf(TPP)_2]^{2+}$: 131618-84-3

---

[1] Part LX: J. W. Buchler, P. Hammerschmitt, *Liebigs Ann. Chem.* **1991**, 1177.

[2] Abbreviations used: C, Coulomb; H(acac), acetylacetone; F, Faraday; Ln, lanthanoid metal; M, metal; NIR, near infrared; OM, Oxidation State Marker Band; SCE, KCl-saturated calomel electrode; tBu_2NO, di-*tert*-butylnitroxyl; TCB, 1,2,4-trichlorobenzene.

[3] [3a] J. W. Buchler, H. G. Kapellmann, M. Knoff, K. L. Lay, S. Pfeifer, *Z. Naturforsch., Teil B,* **38** (1983) 1339. – [3b] J. W. Buchler, A. De Cian, J. Fischer, M. Kihn-Botulinski, H. Paulus, R. Weiss, *J. Am. Chem. Soc.* **108** (1986) 3652. – [3c] J. W. Buchler, A. de Cian, J. Fischer, P. Hammerschmitt, J. Löffler, B. Scharbert, R. Weiss, *Chem. Ber.* **122** (1989) 2219.

[4] O. Bilsel, J. Rodriguez, D. Holten, *J. Phys. Chem.* **94** (1990) 3508.

[5] [5a] G. S. Girolami, S. N. Milam, K. S. Suslick, *Inorg. Chem.* **26** (1987) 343. – [5b] G. S. Girolami, S. N. Milam, K. S. Suslick, *J. Am. Chem. Soc.* **110** (1988) 2011. – [5c] O. Bilsel, J. Rodriguez, D. Holten, G. S. Girolami, S. N. Milam, K. S. Suslick, *J. Am. Chem. Soc.* **112** (1990) 4075.

[6] [6a] J. W. Buchler, A. De Cian, J. Fischer, P. Hammerschmitt, R. Weiss, *Chem. Ber.* **124** (1991) 1051. – [6b] P. Hammerschmitt, *Dissertation,* Technische Hochschule Darmstadt, 1990. – [6c] O. Bilsel, J. W. Buchler, P. Hammerschmitt, J. Rodriguez, D. Holten, *Chem. Phys. Lett.* **182** (1991) 415.

[7] K. Kim, W. S. Lee, H.-J. Kim, S.-H. Cho, G. S. Girolami, P. A. Gorlin, K. S. Suslick, *Inorg. Chem.* **30** (1991) 2652.

[8] Further details of the crystal structure determination are available on request from the Fachinformationszentrum Karlsruhe, Gesellschaft für wissenschaftlich-technische Informationen mbH, D-7514 Eggenstein-Leopoldshafen 2, on quoting the depository number CSD-55569, names of the authors, and the journal citation.

[9] W. R. Scheidt, Y. J. Lee, *Struct. Bonding (Berlin)* **64** (1987) 1.

[10] [10a] J. W. Buchler, K. Elsässer, M. Kihn-Botulinski, B. Scharbert, *Angew. Chem.* **98** (1986) 257; *Angew. Chem. Int. Ed. Engl.* **25** (1986) 286. – [10b] J. W. Buchler, *Comments Inorg. Chem.* **6** (1987) 175.

[11] [11a] J. W. Buchler, B. Scharbert, *J. Am. Chem. Soc.* **110** (1988) 4272. – [11b] M. Kihn-Botulinski, *Dissertation,* Technische Hochschule Darmstadt, 1986. – [11c] J. W. Buchler, J. Hüttermann, J. Löffler, *Bull. Chem. Soc. Jpn.* **61** (1988) 71. – [11d] J. W. Buchler, A. De Cian, J. Fischer, M. Kihn-Botulinski, R. Weiss, *Inorg. Chem.* **27** (1988) 339. – [11e] J. W. Buchler, M. Kihn-Botulinski, B. Scharbert, *Z. Naturforsch., Teil B,* **43** (1988) 1371. – [11f] J. W. Buchler, J. Löffler, *Z. Naturforsch., Teil B,* **45** (1990) 531.

[12] J. W. Buchler, P. Hammerschmitt, I. Kaufeld, J. Löffler, *Chem. Ber.* **124** (1991) 2151.

[13] J. W. Buchler, M. Kihn-Botulinski, J. Löffler, B. Scharbert, *New J. Chem.*, in press.

[14] [14a] J.-H. Fuhrhop, P. Wasser, D. Riesner, D. Mauzerall, *J. Am. Chem. Soc.* **94** (1972) 7996. – [14b] R. H. Felton, D. Dolphin, D. C. Borg, J. Fajer, *J. Am. Chem. Soc.* **91** (1969) 196. – [14c] H. Song, R. D. Orosz, C. A. Reed, W. R. Scheidt, *Inorg. Chem.* **29** (1990) 4274.

[15] R. Guilard, A. Dormond, M. Belkalem, J. E. Anderson, Y. H. Liu, K. M. Kadish, *Inorg. Chem.* **26** (1987) 1410.

[16] E. T. Shimomura, M. A. Phillippi, H. M. Goff, W. F. Scholz, C. A. Reed, *J. Am. Chem. Soc.* **103** (1981) 6778.

[17] [17a] R. J. Donohoe, J. K. Duchowski, D. F. Bocian, *J. Am. Chem. Soc.* **110** (1988) 6119. – [17b] J. K. Duchowski, D. F. Bocian, *J. Am. Chem. Soc.* **112** (1990) 3312. – [17c] J.-H. Perng, J. K. Duchowski, D. F. Bocian, *J. Phys. Chem.* **94** (1990) 6684. – [17d] J. K. Duchowski, D. F. Bocian, *Inorg. Chem.* **29** (1990) 4158. – [17e] J. K. Duchowski, D. F. Bocian, *J. Am. Chem. Soc.* **112** (1990) 8807.

[18] F. Yamauchi, R. W. Kreilick, *J. Am. Chem. Soc.* **91** (1969) 3429.

[19] J. C. Marchon, A. T. Chang, *Inorg. Chim. Acta* **53** (1981) 241.

[20] H. Lueken, J. W. Buchler, K. L. Lay, *Z. Naturforsch., Teil B,* **31** (1976) 1596.

[21] B. A. Frenz, The Enraf-Nonius CAD4-SDP in *Computing in Crystallography* (H. Schenk, R. Olthoff-Hazekamp, H. van Koningveld, G. C. Bassi, Eds.), p. 64–71, Delft University Press 1978.

[22] M. S. Lehmann, F. K. Larsen, *Acta Crystallogr., Sect. A,* **30** (1974) 580.

[23] N. Walker, D. Stuart, *Acta Crystallogr., Sect. A,* **39** (1983) 158.

[24] [24a] D. T. Cromer, J. T. Waber, *International Tables for X-ray Crystallography*, vol. IV, The Kynoch Press, Birmingham 1974, Table 2.2b. – [24b] Ref.[24a], Table 2.3.1.

[282/91]